Nonadiabatic effects in periodically driven dissipative open quantum systems

Reimer, V.; Pedersen, K.G.L.; Tanger, N.; Pletyukhov, M.; Gritsev, V.

DOI
10.1103/PhysRevA.97.043851
Publication date
2018
Document Version
Final published version
Published in
Physical Review A

Nonadiabatic effects in periodically driven dissipative open quantum systems

Viktor Reimer,[1] Kim G. L. Pedersen,[1] Niklas Tanger,[1] Mikhail Pletyukhov,[1] and Vladimir Gritsev[2,3]
[1]*Institute for Theory of Statistical Physics, RWTH Aachen University, 52056 Aachen, Germany*
[2]*Institute for Theoretical Physics, Universiteit van Amsterdam, 1098 XH Amsterdam, The Netherlands*
[3]*Russian Quantum Center, 143025 Skolkovo (Moscow), Russia*

(Received 23 February 2018; published 20 April 2018)

We present a general method to calculate the periodic steady state of a driven-dissipative system coupled to a transmission line (and more generally, to a reservoir) under periodic modulation of its parameters. Using Floquet's theorem, we formulate the differential equation for the system's density operator which has to be solved for a single period of modulation. On this basis we also provide systematic expansions in both the adiabatic and high-frequency regime. Applying our method to three different systems—two- and three-level models as well as the driven nonlinear cavity—we propose periodic modulation protocols of parameters leading to a temporary suppression of effective dissipation rates, and study the arising nonadiabatic features in the response of these systems.

DOI: 10.1103/PhysRevA.97.043851

I. INTRODUCTION

Classical Floquet theory [1] gave long-standing inspiration for studies of a variety of time-periodic processes in nature and has found a huge domain of applicability in fields ranging from dynamical system theory to technology. In quantum mechanics, Bloch's theorem for crystals [2] represents the momentum-space analog of Floquet's seminal work, while in the time domain the concept of quasienergy was introduced only in the 1960s by Zeldovich [3].

Periodic time-dependent processes are natural in quantum optics where the input laser field provides a fast periodic driving of the system. To the best of our knowledge, it was Shirley [4] who first applied a Floquet formalism in quantum optics. He clarified the connection between a semiclassical external field drive and its strong, quantized, resonant single-mode field counterpart applied to an N-level atom based on general considerations using Floquet's theorem. Various extensions of this work, which focused on the semiclassical picture suggested by the strong-intensity nature of laser fields have been reviewed in Refs. [5–7].

In the quantum regime, studies of periodically driven dissipative (open) quantum systems—immediately relevant for quantum optics—have led to a whole new class of physics inaccessible in equilibrium systems. Most of the earlier developments are reviewed in Refs. [8,9], including the paradigmatic two-level systems, tunneling problems, and spin-boson models. More recent examples with potential for technological applications cover the emergence of topological phases—the so-called Floquet topological insulators [10]—nonthermal steady states exhibiting localization [11], and artificial gauge systems [12].

A particularly useful approach for studying driven dissipative systems is the so-called Floquet–Liouvillie approach [13] which reduces to a Lindbladian master equation under the Floquet–Markov approximation [14]. We note that there is a subtlety concerning different procedures of performing the Markovian approximation. In general, the Markovian approximation for the eigenenergy spectrum performed on the level of the undriven Hamiltonian differs from performing it on the level of the driven Floquet quasienergy spectrum. Applications of such approaches, which have been shown to capture some interesting features of periodically driven dissipative quantum systems, range from transport problems such as electronic pumping [15] to dynamical decoupling schemes for qubit control [16]; see also Ref. [17] for a review. However, due to the large separation of system and driving timescales—a regime where the Markovian approximation is very well valid—it has been most widely applied in the context of quantum optics; see, e.g., Refs. [18–25].

Recently, there has been increasing interest in investigating driven dissipative phase transitions where the Liouvillian gap is generically suppressed. For example, the phase transition of the open Rabi model [26] gives rise to long lived metastable states [27]. We will later focus on a different system exhibiting a dissipative phase transition, the Kerr-nonlinearity model, which has been analytically solved for the time-independent stationary case by Drummond and Walls [28] in the 1980s. It has been shown experimentally, that the bistable behavior of Kerr nonlinearities can be exploited to confine the manifold of available states in superconducting qubits to coherent states under special two-photon driving schemes [29]. Since then, driving of this model has been subject to extensive theoretical studies [30–33].

Analytical investigations employing the Floquet–Liouville approach are in practice restricted to either adiabatic or high-frequency limits, and only for few problems [34,35] it is feasible to derive closed systems of equations. Whereas for closed systems the high-frequency Magnus expansion is typically—and successfully—used [36], the complex eigenenergies characteristic for open systems prohibit any truncation of the Magnus series because it typically yields exponentially increasing (i.e., unphysical) terms. On the other hand, an adiabatic approximation may be invalid even for slow driving frequencies if the effective dissipation rate is (temporarily)

suppressed. This will be the case for models discussed in this paper and we show that *nonadiabatic effects* become prominent even when the modulation is slow compared with bare dissipation rates.

In this paper, we establish a general framework for studying the periodic steady state in the long-time regime of periodically driven-dissipative quantum systems that is capable of systematically addressing both slow and fast modulations. It extends the previously developed method based on the scattering formalism [37], allowing us to capture multiphoton processes via the equation of motion approach. The latter is designed in such a way that an integration is required over a single period of modulation only. The adiabatic and high-frequency limits can therefore be efficiently benchmarked against exact numerical results. We apply our framework to investigate nonadiabatic effects which in general arise due to a nearly vanishing Liouvillian gap. These effects can appear useful for implementing adiabatic quantum computation with superconducting qubits coupled to baths [38], and for various dynamical decoupling schemes [39].

We apply our approach to three quantum optical systems exhibiting a critical suppression of the smallest dissipation rate. In Sec. IV, a two-level system with a periodically driven coupling to the transmission line is considered. This model exhibits the striking feature of alternating in time between bunching and antibunching statistical behavior of reflected photons.

In Sec. V we show that similar nonadiabatic effects can be realized with a three-level Λ system when the drive-field intensity is periodically modulated.

Finally, in Sec. VI we consider the Kerr-nonlinearity model where we focus on the system's response to changing parameters across the region of the dissipative phase transition and the emergence of the hysteretic behavior which has been recently theoretically predicted [32] and experimentally observed [33].

II. MODEL

The models considered within this paper all share the notion of a quantum system described by the local Hamiltonian $H_s(t)$ which is driven via a coupled transmission line, or waveguide, by a coherent pulse $|\Psi_0\rangle$ characterized in terms of the photonic flux f, as shown in Fig. 1. The whole setup is described by the Hamiltonian

$$H(t) = H_s(t) + H_w + H_c(t), \tag{1}$$

with the waveguide contribution $H_w = \sum_\alpha \int d\omega(\omega_0 + \omega) a^\dagger_{\alpha\omega} a_{\alpha\omega}$ written in terms of left- and a right-propagating fields labeled by mode (ω) and direction ($\alpha = L, R$) indices. We either assume a time-dependent coupling strength $g(t)$ in the coupling Hamiltonian

$$H_c(t) = \sum_\alpha \int d\omega \left[\frac{g(t)}{\sqrt{2}} a^\dagger_{\alpha\omega} O + \text{H.c.} \right], \tag{2}$$

where O is some operator of the local system, or a periodic modulation of some parameters of the local quantum system Hamiltonian $H_s(t)$ itself.

The form of H_w implies the general assumption that the dispersion of the transmission line can be linearized around a working frequency ω_0, such that $\omega_k = v(k - k_0) + \omega_0$, where v is the group velocity. For convenience, we employ units in which $v = \hbar = 1$ holds. Extending the linearized dispersion to the full spectrum is known as the wide-band approximation and is valid if the working frequency ω_0 is large compared with all other energy scales, including the driving frequency, $\omega_0 \gg \Omega$, and nearly resonant with a transition in the local system described by the operator O. Note that this also falls in line with neglecting counter-rotating terms in the rotating wave approximation (RWA) leading to the coupling Hamiltonian (2) and effectively constitutes the Markovian limit which holds even in the case of time-periodic modulation as is shown in the appendix.

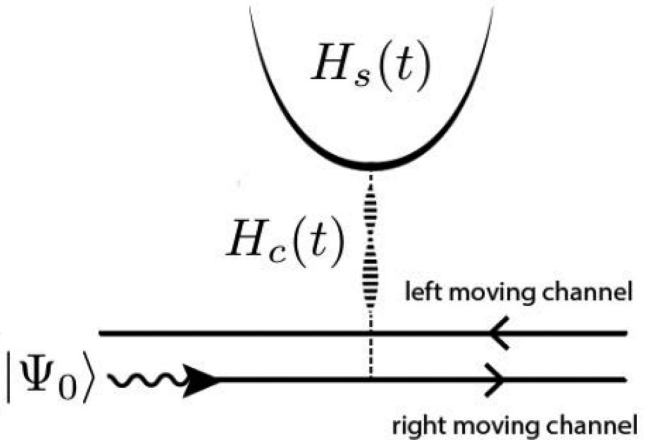

FIG. 1. Open quantum system model: A local system is coupled to a transmission line supporting left- and right-propagating modes. Either the system's parameters or its coupling to the transmission line is periodically modulated. The input pulse into the transmission line is given by a coherent state $|\Psi_0\rangle$ in the right-propagating mode ω_0. The pulse's intensity is characterized by the photonic flux f.

Time dynamics of the system's reduced density matrix is then governed by the Lindblad master equation

$$\dot\rho(t) = -i[H_{\text{eff}}(t), \rho(t)] + \gamma(t)\mathcal{D}[O]\rho(t), \tag{3}$$

with a time-dependent dissipation rate $\gamma(t) \equiv \pi |g(t)|^2$, and

$$H_{\text{eff}}(t) = H_s(t) + \sqrt{\pi f}\, g(t) O + \sqrt{\pi f}\, g^*(t) O^\dagger, \tag{4}$$

$$\mathcal{D}[O]\rho(t) = O\rho(t)O^\dagger - \tfrac{1}{2} O^\dagger O \rho(t) - \tfrac{1}{2}\rho(t) O^\dagger O. \tag{5}$$

III. PERIODIC STEADY-STATE FORMALISM

The aim of this section is to set up a formalism which allows us to directly access the periodic steady-state solution of Eq. (3) in the long-time limit by using Floquet's theorem in the time representation. Traditionally (see, e.g., Ref. [27], for a recent application), Floquet's theorem is employed to get rid of an explicit time dependence of periodic Hamiltonians or Liouvillians by switching to the Fourier representation. The problem is thereby reduced to a static eigenvalue problem for the so-called Floquet quasienergies and modes in an enlarged Hilbert space. While this procedure is in principle always possible, it introduces certain difficulties for practical numerical calculations, since it necessitates a truncation of the

infinite number of Floquet modes. This is especially perilous if an additional cutoff, e.g., in the Fock basis, is required, such as, for example, in the case of the Kerr-nonlinearity model considered in Sec. VI. For this reason, we prefer a formulation in terms of differential equations for periodic steady states which can be solved on a single period of modulation.

The starting point of our consideration is the master equation for the reduced density operator $\rho(t)$ of the local system,

$$\frac{d}{dt}\rho(t) = -iL(t)\rho(t), \tag{6}$$

with the Liouvillian superoperator $L(t)$ generalizing the one in Eq. (3). In spite of the time dependence, it must have a zero eigenvalue, as it is dictated by the trace preservation of $\rho(t)$. It is convenient to explicitly split off the corresponding zero eigenmode of $L(t)$. To do so, we fix some matrix representation of $\rho(t)$ and express the occupation probability of the ground state by $\rho_{00}(t) = 1 - \sum_{i=1}^{N-1} \rho_{ii}(t)$, where N is the number of states in the system. In the vectorized form, i.e., by restacking the columns of the matrix representation of $\rho(t)$ into an N^2-dimensional vector $(\rho_{00}, \vec{\rho})^T$, the master equation (6) turns into

$$\frac{d}{dt}\begin{pmatrix}\rho_{00}(t)\\ \vec{\rho}(t)\end{pmatrix} = \begin{pmatrix}-iL_{00}(t) & \vec{\bar{C}}^T(t)\\ \vec{C}(t) & -i\bar{L}(t)\end{pmatrix}\begin{pmatrix}\rho_{00}(t)\\ \vec{\rho}(t)\end{pmatrix}. \tag{7}$$

As a result, all information has been encoded in the (N^2-1)-dimensional state vector $\vec{\rho}(t)$ governed by the differential equation

$$\begin{aligned}\frac{d}{dt}\vec{\rho}(t) &= [-\vec{C}(t)\otimes\vec{E}^T - i\bar{L}(t)]\vec{\rho}(t) + \vec{C}(t)\\ &\equiv A(t)\vec{\rho}(t) + \vec{C}(t),\end{aligned} \tag{8}$$

where $\vec{E}$ consists of ones (zeros) in the positions corresponding to the diagonal (off-diagonal) elements of $\vec{\rho}$.

For a time-independent Liouvillian, Eq. (8) allows for a direct calculation of the true stationary state $\vec{\rho}_{\rm st} = -A^{-1}\vec{C}$. In the case of a time-periodic driving, time translational invariance is lost even in the long-time limit and the time-periodic steady state $\vec{\rho}_{\rm ps}(t)$ will essentially follow the persistent external modulation after some transient time regime in which the influence of the initial state gradually decays. We are interested in this long-time limit and take the initial time $t_0 = -M_0 T \to -\infty$ to be in the far past, where we assume without loss of generality that it is back by a large integer multiple $M_0 \gg 1$ of the driving period T. The ansatz

$$\vec{\rho}(t) = \lim_{t_0\to-\infty} O(t)\vec{\rho}(t_0) + \vec{\rho}_{\rm ps}(t) \tag{9}$$

reflects the split structure of Eq. (8) and gives a clear physical interpretation of the appearing vectors and matrices.

The matrix $O(t)$ describes the gradual decay of the initial conditions in the far past and is solely governed by the periodic matrix $A(t)$,

$$\dot{O}(t) = A(t)O(t), \quad O(0) = \mathbb{1}. \tag{10}$$

Note that the reference time has been shifted from t_0 to zero which is possible here due to the periodic nature of $A(t)$. According to Floquet's theorem, the solution of this differential equation can be represented as

$$O(t) = P(t)e^{Bt}, \tag{11}$$

where $P(t) = P(t+T)$ is a periodic matrix function with the initial condition $P(0) = \mathbb{1}$. The constant matrix B, which is obtained from the monodromy matrix $O(T) = P(T)e^{BT} = e^{BT}$, has eigenvalues with negative real parts such that $\lim_{t\to\infty} O(t) = 0$ holds, and all information about initial conditions in Eq. (9) is lost, as required.

After the initial conditions have fully decayed, only the periodic steady-state vector $\vec{\rho}_{\rm ps}(t)$ remains. It is governed by the differential equation

$$\dot{\vec{\rho}}_{\rm ps}(t) = A(t)\vec{\rho}_{\rm ps}(t) + \vec{C}(t), \quad \lim_{t_0\to-\infty}\vec{\rho}_{\rm ps}(t_0) = 0, \tag{12}$$

where, unlike in the case of $O(t)$, the reference time t_0 remains unaltered to account for the fact that we are interested in the long-time limit. The differential equation (12) can be formally integrated to

$$\vec{\rho}_{\rm ps}(t) = O(t)\int_{-\infty}^{t} dt' O^{-1}(t')\vec{C}(t'). \tag{13}$$

The periodicity of this solution is straightforwardly seen from Eq. (11) and the periodicity of $P(t)$ and $\vec{C}(t)$, and therefore it is sufficient to study its behavior on the finite interval $\tau_c \in [0,T]$.

To further evaluate Eq. (13), we first split the integration range into two intervals $[-\infty,0]$ and $[0,\tau_c]$,

$$\vec{\rho}_{\rm ps}(\tau_c) = O(\tau_c)\int_{-\infty}^{0} dt' O^{-1}(t')\vec{C}(t') + \vec{c}(\tau_c), \tag{14}$$

where

$$\vec{c}(\tau_c) = O(\tau_c)\int_{0}^{\tau_c} dt' O^{-1}(t')\vec{C}(t') \tag{15}$$

is defined in analogy with Eq. (13) with the reference time shifted to zero. We note that instead of inverting the large matrix $O(t)$ appearing in Eq. (15), it is more favorable to instead numerically solve the differential equation

$$\dot{\vec{c}}(t) = A(t)\vec{c}(t) + \vec{C}(t), \quad \vec{c}(0) = 0. \tag{16}$$

Next, the interval $[-\infty,0]$ is split into an infinite number of intervals $[-(n+1)T,-nT]$, $n \in \mathbb{N}_0$. Using the periodicity of $P(t)$, we represent the first term of Eq. (14) by a geometric progression with the factor e^{BT}. Resumming it, we obtain

$$\vec{\rho}_{\rm ps}(\tau_c) = O(\tau_c)[1 - O(T)]^{-1}\vec{c}(T) + \vec{c}(\tau_c). \tag{17}$$

Thus, to evaluate $\vec{\rho}_{\rm ps}(t)$, it is sufficient to solve the set of equations (10) and (16) on the finite interval $0 \leqslant \tau_c \leqslant T$. In fact, the solution (17) obeys the differential equation (12) with periodic boundary conditions rather than the initial condition therein.

A. Adiabatic expansion

In the adiabatic limit, the external driving of parameters is sufficiently slow such that the state can instantaneously adapt to its new environment, $\rho_{\rm ps}(t) \approx -A^{-1}(t)\vec{C}(t) \equiv \rho_{\rm inst}(t)$.

To consistently compute adiabatic corrections to the instantaneous solution $\rho_{\rm inst}(t)$, we insert the relation $O^{-1}(t) = -\frac{d}{dt}[O^{-1}(t)]A^{-1}(t)$ into Eq. (13). Integrating it by parts we obtain

$$\vec{\rho}_{\rm ps}(t) = \rho_{\rm inst}(t) - O(t)\int_{-\infty}^{t} dt' O^{-1}(t')\frac{d}{dt'}\rho_{\rm inst}(t'). \tag{18}$$

Iterating this procedure leads to a geometric series that can be resummed to

$$\vec{\rho}_{\rm ps}(t) = \frac{1}{1 - A^{-1}(t)\frac{d}{dt}}\vec{\rho}_{\rm inst}(t) \approx \vec{\rho}_{\rm inst}(t) + A^{-1}(t)\frac{d}{dt}\vec{\rho}_{\rm inst}(t). \quad (19)$$

We note that the convergence of this series relies on some sort of an adiabaticity condition. If such a condition is violated or generally not provided, the adiabatic expansion (19) breaks down.

B. High-frequency expansion

The Magnus expansion is frequently used for analyzing high-frequency processes in driven quantum optical systems. Note, however, that it is originally designed for applications in closed systems where the evolution is unitary. For driven dissipative systems with Liouvillian dynamics, it often produces—according to our experience—exponentially growing, unphysical terms already in the first order of expansion.

Instead of the Magnus expansion, we perform a straightforward high-frequency expansion of the master equation (8) in the following way: Since in the long-time limit $A(t)$, $\vec{C}(t)$, and $\vec{\rho}(t)$ are all periodic functions of time, let us explicitly split off the constant zero-frequency component for each of these objects:

$$X(t) = \overline{X} + \widetilde{X}(t), \quad \overline{X} = \frac{1}{T}\int_0^T dt' X(t'). \quad (20)$$

Here $\widetilde{X}(t)$ is a periodic function with zero time average. Then, we rewrite the master equation (8), which must also hold in the long-time limit with periodic boundary conditions, as (vector notation omitted in the following)

$$\frac{d}{dt}\widetilde{\rho}(t) = (\overline{A} + \widetilde{A}(t))\overline{\rho} + (\overline{A} + \widetilde{A}(t))\widetilde{\rho}(t) + \overline{C} + \widetilde{C}(t). \quad (21)$$

The constant average $\overline{\rho}$ can be expressed in terms of the periodic part $\widetilde{\rho}$ if one integrates Eq. (21) over one period,

$$\overline{\rho} = -\overline{A}^{-1}\left(\overline{C} + \frac{1}{T}\int_0^T dt' \widetilde{A}(t')\widetilde{\rho}(t')\right). \quad (22)$$

Now, perform a high-frequency expansion of $\rho(t)$ in powers of the inverse modulation frequency $\Omega = 2\pi/T$:

$$\overline{\rho} = \sum_{n=0}^{\infty}\frac{1}{\Omega^n}\overline{\rho}^{(n)}, \quad \widetilde{\rho}(t) = \sum_{n=1}^{\infty}\frac{1}{\Omega^n}\widetilde{\rho}^{(n)}(t). \quad (23)$$

The hierarchy of differential equations resulting from this ansatz,

$$\frac{d}{dt}\widetilde{\rho}^{(1)}(t) = \widetilde{A}(t)\overline{\rho}^{(0)} + \widetilde{C}(t), \quad (24a)$$

$$\frac{d}{dt}\widetilde{\rho}^{(n)}(t) = \widetilde{A}(t)\overline{\rho}^{(n-1)} + \overline{A}\,\widetilde{\rho}^{(n-1)}(t) + \widetilde{A}(t)\widetilde{\rho}^{(n-1)}(t) - \frac{1}{T}\int_0^T dt' \widetilde{A}(t')\widetilde{\rho}^{(n-1)}(t'), \quad n \geqslant 2, \quad (24b)$$

can be iteratively solved as follows: First, we extract from Eq. (22) the leading order of the expansion for the constant average,

$$\overline{\rho}^{(0)} = -\overline{A}^{-1}\overline{C}, \quad (25)$$

with which we can formally solve Eq. (24a):

$$\widetilde{\rho}^{(1)}(t) = -\left(\int_0^t dt' \widetilde{A}(t') - \frac{1}{T}\int_0^T dt \int_0^t dt' \widetilde{A}(t')\right)\overline{A}^{-1}\overline{C} + \int_0^t dt' \widetilde{C}(t') - \frac{1}{T}\int_0^T dt \int_0^t dt' \widetilde{C}(t'). \quad (26)$$

Knowing $\widetilde{\rho}^{(1)}(t)$, we can then also extract $\overline{\rho}^{(1)}$ from Eq. (22):

$$\overline{\rho}^{(1)} = -\overline{A}^{-1}\frac{1}{T}\int_0^T dt' \widetilde{A}(t')\widetilde{\rho}^{(1)}(t'). \quad (27)$$

The higher-order contributions are obtained by an analogous iterative procedure.

IV. DRIVEN TWO-LEVEL SYSTEM

Here we apply the Floquet formalism developed above to a setup in which the local quantum system has two levels (a qubit) and the coupling to the transmission line is periodically modulated. We have already discussed this setup in the recent publication [37] in the regime of weak intensities $f \ll \gamma$ of the coherent input pulse using Floquet scattering theory. The present approach allows us to extend our previous results to larger input powers $f \geqslant \gamma$.

The Hamiltonian (1) of this system is specified by $H_s(t) = \omega_e\sigma_+\sigma_-$ and $O = \sigma_-$. Going to the co-rotating frame, we find that the master equation (8) for $\vec{\rho}(t) \to \vec{s}(t) = \langle\hat{\vec{s}}(t)\rangle \equiv (\langle\tilde{\sigma}_+(t)\rangle, \langle\tilde{\sigma}_-(t)\rangle, \langle 1 + \sigma_z(t)\rangle)^T$ uses

$$A(t) = \begin{pmatrix} -i\delta - \gamma(t)/2 & 0 & -i\sqrt{\pi f}\,g(t) \\ 0 & i\delta - \gamma(t)/2 & i\sqrt{\pi f}\,g^*(t) \\ -2i\sqrt{\pi f}\,g^*(t) & 2i\sqrt{\pi f}\,g(t) & -\gamma(t) \end{pmatrix}, \quad (28)$$

and

$$\vec{C}(t) = (i\sqrt{\pi f}\,g(t), -i\sqrt{\pi f}\,g^*(t), 0)^T. \quad (29)$$

Here we introduced the detuning $\delta = \omega_0 - \omega_e$ as well as $\langle\tilde{\sigma}_\mp(t)\rangle = \langle\sigma_\mp(t)\rangle e^{\pm i\omega_0(t-t_0)}$.

Importantly, in a broad range of f, the smallest dissipation rate is solely determined by the coupling strength g, and quenching $g \to 0$ will cause a critical slowing down of the system's Liouvillian dynamics. We exploit this property to design a modulation protocol $g(t)$ aiming to achieve time intervals where the modulation frequency $\Omega = 2\pi/T$ exceeds the scale set by the smallest dissipation rate, $\Omega > \gamma_{\rm min}(t)$. Within these time intervals, we expect the system's response to be nonadiabatic such that the expansion (19) breaks down.

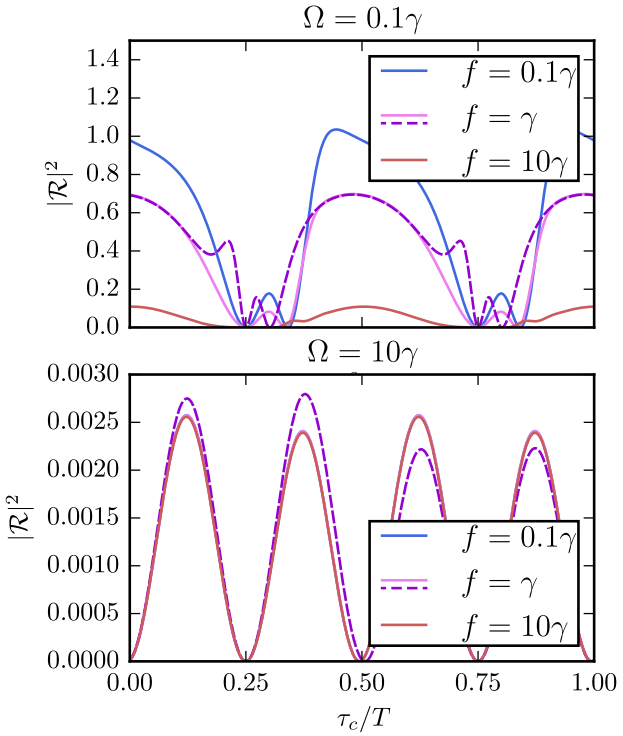

FIG. 2. Reflection from the qubit on resonance, $\delta = 0$, for the time-modulated coupling $g(t) = g_0 \cos \Omega t$ with slow $\Omega = 0.1\gamma$ (top) and fast $\Omega = 10\gamma$ (bottom) modulation frequencies, expressed in the units of $\gamma = \pi g_0^2$. (top) The adiabatic approximation (dashed line) obtained from Eq. (19) deviates from the numerical solution in the vicinities of time instants when the coupling is quenched. For all values of f, the reflection is suppressed at these points. At large f, the reflection is completely suppressed because of the qubit's saturation. (bottom) The high-frequency modulation suppresses the reflection for any input power f. The numerical result (solid lines) is well approximated by the high-frequency result (dashed line) obtained from Eqs. (25)–(27).

A. Reflection and transmission

Applying the standard input-output relations (cf. Appendix), we find reflection and transmission amplitudes

$$\mathcal{R}(t) \equiv \frac{\langle a_{L,\mathrm{out}}(t)\rangle}{\langle a_{R,\mathrm{in}}(t)\rangle} = -i\sqrt{\frac{\pi}{f}}\, g(t) s_2(t), \tag{30}$$

$$\mathcal{T}(t) \equiv \frac{\langle a_{R,\mathrm{out}}(t)\rangle}{\langle a_{R,\mathrm{in}}(t)\rangle} = 1 + \mathcal{R}(t), \tag{31}$$

which are expressed via the second component of the vector $\vec{s}(t)$.

The numerically obtained reflection $|\mathcal{R}|^2(\tau_c)$ in the periodic steady state with a cosinusoidal modulation of $g(t)$ is shown in Fig. 2 for different input powers f on a single period T. The results for weak input powers are equivalent to those obtained by the Floquet scattering approach in Ref. [37]. This is confirmed analytically by perturbatively evaluating Eq. (13) in the weak power limit $f \ll |\bar{\gamma} - i\bar{\delta}|$. Obtaining

$$s_{\mathrm{ps},2}(t) \approx -i\sqrt{\pi f}\, e^{-F(t)} \int_{-\infty}^{t} dt' e^{F(t')} g^*(t'),$$

with $F(t) = \int_0^t dt'[\gamma(t') - i\delta(t')]$, we exactly reproduce the reflection amplitude given in Eq. (34) of Ref. [37].

We note that, for the modulation protocol $g(t) = g_0 \cos \Omega t$, where the coupling periodically switches its sign, the period of the steady-state reflection (shown in Fig. 2) is exactly half of the modulation period T. Moreover, reflection goes to zero not only at the quench times when $g(t) = 0$ but also at some intermediate times. Remarkably, the adiabaticity is violated around the quench points even at sufficiently slow modulation, as one can conclude from the comparison (see the upper panel) of the numerical solution (solid line) for $f = \gamma \equiv \pi g_0^2$ with the corresponding adiabatic approximation of Sec. III A (dashed line). This feature has already been noticed previously in Ref. [37] for weak input powers f, and now we see that it persists with increasing f. In the beginning ($\tau_c \approx 0$), in the middle ($\tau_c \approx T/2$), and in the end ($\tau_c \approx T$) of the modulation period, the instantaneous relaxation rate $\gamma(t)$ is larger than Ω, and the adiabatic approximation approaches the numerical result. The overall decrease of the reflection with increasing f is naturally associated with the qubit's saturation.

In contrast to the adiabatic approximation, the high-frequency approximation at fast modulations, introduced in Sec. III B, is most accurate in the vicinities of the quench points, as follows from its comparison (dashed line) with the numerical solution (solid lines) in the lower panel of Fig. 2. In general, fast modulation tends to suppress the reflection for any value of the input power f.

B. Power spectrum

The power spectrum is related to the correlation function of outgoing photons,

$$\begin{aligned} g_\alpha^{(1)}(\tau,\tau_c) &= \langle a_{\alpha,\mathrm{out}}^\dagger(\tau_c+\tau) a_{\alpha,\mathrm{out}}(\tau_c)\rangle \\ &= \delta_{\alpha,L} e^{i\omega_0\tau} f \mathcal{R}^*(\tau_c+\tau)\mathcal{R}(\tau_c) && \text{(32a)} \\ &\quad + \delta_{\alpha,R} e^{i\omega_0\tau} f \mathcal{T}^*(\tau_c+\tau)\mathcal{T}(\tau_c) && \text{(32b)} \\ &\quad + e^{i\omega_0\tau}\pi g^*(\tau_c+\tau) g(\tau_c) G_1(\tau,\tau_c), && \text{(32c)} \end{aligned}$$

where the terms (32a) and (32b) give rise to the elastic contribution to the power spectrum for reflected and transmitted photons, respectively, while the common term (32c) constitutes the inelastic contribution.

A proper definition of the power spectrum requires time-translational invariance, which can be restored in the periodic steady state by averaging the variable $\tau_c \in [0,T]$ over a period of modulation. With the Fourier expansion $\mathcal{R}(\tau_c) = \sum_m \mathcal{R}^{(m)} e^{-im\Omega\tau_c}$ of the steady-state reflection (and, equivalently, transmission) amplitude, we hence obtain for the elastic contribution

$$\begin{aligned} S_{L,\mathrm{el}}(\omega) &= \frac{1}{2\pi}\int_{-\infty}^{\infty} d\tau \left[\frac{1}{T}\int_0^T d\tau_c\, g_{L,\mathrm{el}}^{(1)}(\tau,\tau_c)\right] e^{-i\omega\tau} \\ &= f\sum_m |\mathcal{R}^{(m)}|^2 \delta(\omega - \omega_0 - m\Omega), \end{aligned} \tag{33}$$

which peaks not only at the working frequency ω_0, but also at frequencies shifted from ω_0 by integer multiples of Ω. An analogous expression holds for $S_{R,\mathrm{el}}(\omega)$ of the transmitted photons with the replacement $\mathcal{R} \to \mathcal{T}$.

Evaluation of the inelastic contribution (32c) to the power spectrum requires knowledge of the vector $\vec{G}(\tau,\tau_c) = \langle \hat{\vec{s}}(\tau_c+\tau)\hat{s}_2(\tau_c)\rangle - \vec{s}_{\rm ps}(\tau_c+\tau)s_{{\rm ps},2}(\tau_c)$ in the long-time limit. We note that only its first component is required, which has the property $G_1(-|\tau|,\tau_c) = G_1(|\tau|,\tau_c)^*$. It is thus sufficient to find an equation for $\vec{G}(\tau,\tau_c)$ by means of the quantum regression theorem for $\tau > 0$ only. It reads

$$\frac{d}{d\tau}\vec{G}(\tau,\tau_c) = A(\tau_c+\tau)\vec{G}(\tau,\tau_c), \tag{34}$$

and its solution can be expressed in terms of $O(t)$ which is governed by the same periodic matrix $A(t)$,

$$\vec{G}(\tau,\tau_c) = O(\tau+\tau_c)O^{-1}(\tau_c)\vec{G}^{(0)}(\tau_c). \tag{35}$$

For the initial condition $\vec{G}(0,\tau_c) = \vec{G}^{(0)}(\tau_c)$, we employ the periodic steady-state values of $\vec{s}_{\rm ps}(\tau_c)$, setting

$$\vec{G}^{(0)}(\tau_c) = \begin{pmatrix} \frac{1}{2}s_{{\rm ps},3}(\tau_c) - |s_{{\rm ps},2}(\tau_c)|^2 \\ -s^2_{{\rm ps},2}(\tau_c) \\ -s_{{\rm ps},3}(\tau_c)s_{{\rm ps},2}(\tau_c) \end{pmatrix}. \tag{36}$$

From the representation $O(t) = P(t)e^{Bt}$ we find for the inelastic contribution

$$\begin{aligned} g^{(1)}_{\alpha,{\rm inel}}(\tau,\tau_c) = {} & \pi e^{i\omega_0\tau}\Theta(\tau)\vec{V}_+(\tau_c+\tau)\cdot e^{B\tau}\vec{V}_0(\tau_c) \\ & + \pi e^{i\omega_0\tau}\Theta(-\tau)[\vec{V}_+(\tau_c)\cdot e^{-B\tau}\vec{V}_0(\tau_c+\tau)]^*, \end{aligned} \tag{37}$$

with the periodic vector functions

$$\vec{V}_+(\tau_c) = g^*(\tau_c)P(\tau_c)\vec{n}_1, \tag{38}$$

$$\vec{V}_0(\tau_c) = g(\tau_c)P^{-1}(\tau_c)\vec{G}^{(0)}(\tau_c), \tag{39}$$

and $\vec{n}_1 = (1,0,0)^T$.

As before, we insert the Fourier expansions for the periodic vectors $\vec{V}_{+,0}(\tau_c) = \sum_m \vec{V}^{(m)}_{+,0}e^{-im\Omega\tau_c}$ to evaluate the τ_c average over a single period of modulation to restore time-translational invariance. Additionally, it is useful to express the matrix $B = \sum_{j=1}^3 b_j \vec{\chi}^{(j)}_r \otimes \vec{\chi}^{(j)}_l$ in terms of its eigenvalues b_j and the corresponding biorthonormal left and right eigenvectors obeying $\vec{\chi}^{(j)}_l \cdot \vec{\chi}^{(j')}_r = \delta_{jj'}$. This gives direct analytical access to resonance positions $\omega_{m,j} = \omega_0 + m\Omega + {\rm Im}\, b_j$ and widths $\sigma_j = -{\rm Re}\, b_j$ in the inelastic power spectrum

$$\begin{aligned} S_{\alpha,{\rm inel}}(\omega) &= \frac{1}{2\pi}\int_{-\infty}^{\infty} d\tau \left[\frac{1}{T}\int_0^T d\tau_c g^{(1)}_{\alpha,{\rm inel}}(\tau,\tau_c)\right]e^{-i\omega\tau} \\ &= \sum_m \sum_{j=1}^3 {\rm Re}\left[\frac{(\vec{V}^{(-m)}_+ \cdot \vec{\chi}^{(j)}_r)(\vec{\chi}^{(j)}_l \cdot \vec{V}^{(m)}_0)}{i(\omega-\omega_0-m\Omega-{\rm Im}\, b_j) - {\rm Re}\, b_j}\right]. \end{aligned} \tag{40}$$

This result indicates equidistant additional resonances introduced by the periodic modulation which can be understood from a dressed-state picture: The periodic modulation further splits the dressed states of the qubit driven through the transmission line into m equidistant Floquet modes. Numerical results shown in Fig. 3 confirm this behavior but also show that, for the modulation protocol $g(t) = g_0\cos\Omega t$, some of the resonances are suppressed and the main peak splits into two side peaks. This behavior can in principle be used for frequency shifting and engineering correlated states of light.

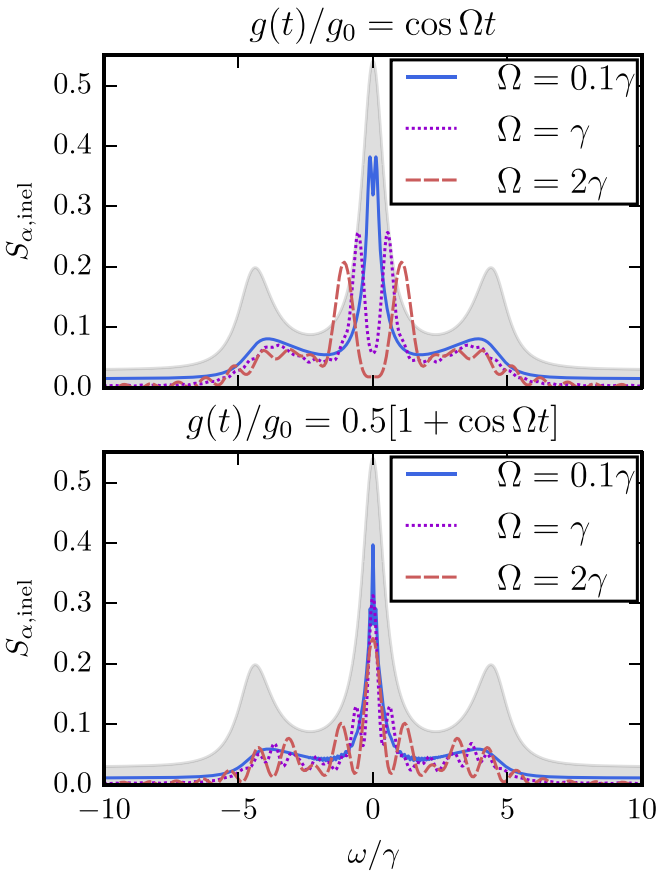

FIG. 3. Inelastic power spectra of the qubit strongly driven ($f = 200\gamma$) on resonance ($\delta = 0$) for the (top) sign-change protocol $g(t) = g_0\cos\Omega t$ and the (bottom) on-off protocol $g(t) = \frac{g_0}{2}(1+\cos\Omega t)$ for various modulation frequencies Ω. The Mollow triplet for the corresponding stationary case at coupling $g = g_0$ is shown for comparison in gray. Additional broadened peaks consistent with the Floquet spectrum arise due to the periodic modulation and may destructively interfere as seen, for example, in the missing main peak in the case of the sign-change protocol (top). Similar features in the power spectrum have been reported in Ref. [40] for a qubit subject to a pulsed excitation.

As a final consistency check, let us confirm the power conservation, i.e., that the output photon fluxes $f_\alpha(\tau_c) = g^{(1)}_\alpha(0,\tau_c)$ average over one period of modulation to give the input flux $f = \bar{f}_L + \bar{f}_R$. In the formal expression, we need to prove the identity

$$\begin{aligned} f &\overset{!}{=} \frac{1}{T}\int_0^T d\tau_c[f_L(\tau_c) + f_R(\tau_c)] \\ &= f - \frac{1}{2T}\int_0^T d\tau_c\left[\sum_{j=1}^3 A_{3,j}(\tau_c)s_{{\rm ps},j}(\tau_c) + C_3(\tau_c)\right] \\ &= f - \frac{1}{2T}\int_0^T d\tau_c \dot{s}_{{\rm ps},3}(\tau_c), \end{aligned} \tag{41}$$

which is indeed fulfilled due to the periodicity of $s_{{\rm ps},3}(\tau_c)$.

C. Second-order coherence function

Statistical properties of scattered photons can be analyzed with help of the second-order coherence function

$$g^{(2)}_{\alpha\alpha}(\tau,\tau_c) = \frac{\langle a^\dagger_{\alpha,\mathrm{out}}(\tau_c) n_{\alpha,\mathrm{out}}(\tau_c+\tau) a_{\alpha,\mathrm{out}}(\tau_c)\rangle}{f_\alpha(\tau+\tau_c) f_\alpha(\tau_c)}, \tag{42}$$

where $n_{\alpha,\mathrm{out}} = a^\dagger_{\alpha,\mathrm{out}} a_{\alpha,\mathrm{out}}$ is the outgoing photon number in channel α. This function has been studied earlier in the context of Floquet scattering theory [37] for weak input powers f, and here we extend those results to larger values of f, for which the scattering theory becomes impractical.

Similar to the procedure of evaluating the power spectrum, the quantum regression theorem allows us to write the functions (42) in terms of the vector

$$\vec{J}(\tau,\tau_c) = \langle \hat{s}_1(\tau_c)\hat{\vec{s}}(\tau+\tau_c)\hat{s}_2(\tau_c)\rangle - \tfrac{1}{2} s_{\mathrm{ps},3}(\tau_c)\vec{s}_{\mathrm{ps}}(\tau+\tau_c), \tag{43}$$

obeying the same differential equation (34) in the variable τ as $\vec{G}(\tau,\tau_c)$ obeys, but with the initial conditions $\vec{J}^{(0)}(\tau_c) = -\frac{1}{2} s_{\mathrm{ps},3}(\tau_c)\vec{s}_{\mathrm{ps}}(\tau_c)$. We find

$$g^{(2)}_{LL}(\tau,\tau_c) = 1 + \frac{2\mathrm{Re}[\nu_3(\tau_c)\nu_3(\tau+\tau_c)J_3(\tau,\tau_c)]}{f_L(\tau+\tau_c)f_L(\tau_c)}, \tag{44a}$$

$$g^{(2)}_{RR}(\tau,\tau_c) = 1 + \frac{2\mathrm{Re}[\nu_3(\tau_c)\vec{\nu}(\tau+\tau_c)\cdot\vec{J}(\tau,\tau_c)]}{f_R(\tau+\tau_c)f_R(\tau_c)} + \frac{2\mathrm{Re}[\nu_2(\tau_c)\vec{\nu}(\tau+\tau_c)\cdot\vec{G}(\tau,\tau_c)]}{f_R(\tau+\tau_c)f_R(\tau_c)}, \tag{44b}$$

where $\vec{\nu}(t) = (0, 0, \frac{1}{4}\gamma(t))^T - \vec{C}^*(t)$ is a modification of the vector (29).

As shown in Fig. 4, the oscillations between strong bunching and antibunching behavior observed in Ref. [37] become less pronounced as the input power f is increased (see the bottom panel of this figure), corresponding to the horizontal (dashed gray) cut in the upper panel. This behavior can again be attributed to the qubit's saturation. For sufficiently fast modulation frequencies ($\Omega \gtrsim \gamma$), the bunching peaks remain sizable on the range of several T in the delay time τ even for the moderate input power $f = 10\gamma$; see the inset of the upper panel corresponding to the vertical (dashed gray) cut of the contour plot.

Thus, the rapid bunching-to-antibunching changes in behavior of the $g^{(2)}$ function, which result from the system's nonadiabatic response to an external modulation and which have been predicted in Ref. [37] for weak input powers f, appear to persist in a broad range of input power f. We observe that the positions of the bunching peaks remain insensitive to f, and only their heights gradually go down with increasing f.

V. DRIVEN Λ SYSTEM

Next, we consider a three-level system in the Λ scheme where a direct transition from the ground state $|g\rangle$ to an intermediate metastable state $|s\rangle$ is forbidden. Such systems are known to exhibit electromagnetically induced transparency (EIT), an effect which was first observed in atomic vapors

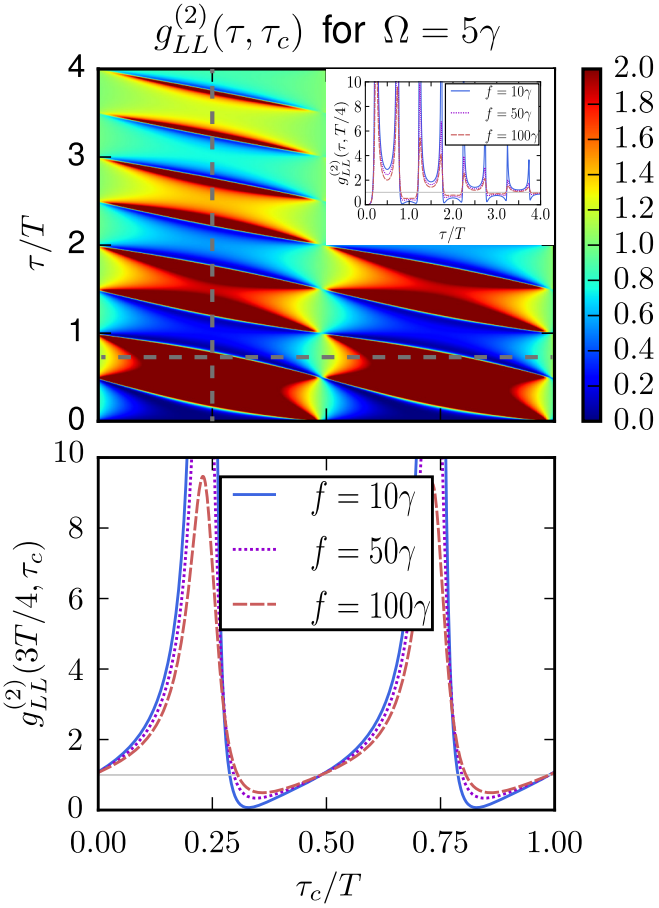

FIG. 4. (top) Second-order coherence function $g^{(2)}_{LL}(\tau,\tau_c)$ for the sign-change protocol $g(t) = g_0\cos(\Omega t)$ of the moderately driven ($f = 10\gamma$) qubit on resonance ($\delta = 0$) at fast modulation frequency $\Omega = 5\gamma$. The oscillations decay with the delay time τ at the rate γ as can be seen, e.g., along the vertical cut at $\tau_c = T/4$ shown in the inset. Thus, this rapidly changing behavior takes place only for sufficiently fast modulations. (bottom) The strong oscillations in time τ_c between bunching and antibunching behavior reported in Ref. [37] become less pronounced with increasing input power f as the qubit becomes saturated. The delay time τ is fixed at the value $3T/4$, which corresponds to the horizontal cut in the top figure.

[41,42]. Recently, this phenomenon has also been demonstrated in superconducting circuits [43], thus paving the way for potential applications in quantum information processing.

The drive field at frequency ω_d, which is nearly resonant with frequency $(\omega_e - \omega_s)$ of the transition $|s\rangle \to |e\rangle$ to the excited state, is conventionally treated classically. Our interest lies in a time modulation of the drive amplitude $F(t)$ causing a periodic switching between opaque and transparent behavior of this system upon irradiation of the coherent probe field $|\Psi_0\rangle$ at frequency ω_0, which is nearly resonant with frequency ω_e of the transition $|g\rangle \to |e\rangle$. This model is described by the Hamiltonian

$$H(t) = \omega_e|e\rangle\langle e| + \omega_s|s\rangle\langle s| + [F(t)e^{-i\omega_d t}|e\rangle\langle s| + \mathrm{H.c.}] + H_w + \sum_\alpha \int d\omega \left[\frac{g}{\sqrt{2}} a^\dagger_{\alpha\omega}|g\rangle\langle e| + \mathrm{H.c.}\right]. \tag{45}$$

In the following, we show that this system exhibits nonadibatic effects similar to those of the two-level system with a modulated coupling strength. At the same time, the Λ-scheme with a periodically modulated drive field is more feasible for an experimental realization.

Dissipative dynamics of the Λ system in the corotating frame is governed by the master equation (8) with the matrix

$$A(t)=\begin{pmatrix} -\gamma & 0 & -i\sqrt{\gamma f/2} & i\sqrt{\gamma f/2} & -iF(t) & iF^*(t) & 0 & 0 \\ 0 & 0 & 0 & 0 & iF(t) & -iF^*(t) & 0 & 0 \\ -2i\sqrt{\gamma f/2} & -i\sqrt{\gamma f/2} & -i(\delta_1-i\gamma/2) & 0 & 0 & 0 & iF^*(t) & 0 \\ 2i\sqrt{\gamma f/2} & i\sqrt{\gamma f/2} & 0 & i(\delta_1+i\gamma/2) & 0 & 0 & 0 & -iF(t) \\ -iF^*(t) & iF^*(t) & 0 & 0 & -i(\delta_2-i\gamma/2) & 0 & 0 & i\sqrt{\gamma f/2} \\ iF(t) & -iF(t) & 0 & 0 & 0 & i(\delta_2+i\gamma/2) & -i\sqrt{\gamma f/2} & 0 \\ 0 & 0 & iF(t) & 0 & 0 & -i\sqrt{\gamma f/2} & -i(\delta_1-\delta_2) & 0 \\ 0 & 0 & 0 & -iF^*(t) & i\sqrt{\gamma f/2} & 0 & 0 & i(\delta_1-\delta_2) \end{pmatrix}, \quad (46)$$

and the vector

$$\vec{C}=(0,0,i\sqrt{\gamma f/2},-i\sqrt{\gamma f/2},0,0,0,0)^T, \quad (47)$$

which are written in the basis

$$\begin{aligned}\vec{s}(t) &= \langle\hat{\vec{s}}(t)\rangle \\ &= (\langle P_e(t)\rangle, \langle P_s(t)\rangle, \langle\tilde{\sigma}_+^{(g)}(t)\rangle, \langle\tilde{\sigma}_-^{(g)}(t)\rangle, \langle\tilde{\sigma}_+^{(s)}(t)\rangle, \\ &\quad \langle\tilde{\sigma}_-^{(s)}(t)\rangle, \langle\tilde{\sigma}_+^{(r)}(t)\rangle, \langle\tilde{\sigma}_-^{(r)}(t)\rangle)^T.\end{aligned}$$

Here, $P_e=|e\rangle\langle e|$, $P_s=|s\rangle\langle s|$, $\sigma_-^{(g)}=|g\rangle\langle e|$, $\sigma_-^{(s)}=|s\rangle\langle e|$, $\sigma_-^{(r)}=|g\rangle\langle s|$, $\sigma_+^{(g,s,r)}=(\sigma_-^{(g,s,r)})^\dagger$, and the tildes indicate expectation values to be evaluated in the corotating frame analogous to the two-level system. Additionally, we have defined the detunings $\delta_1=\omega_0-\omega_e$ and $\delta_2=\omega_d-(\omega_e-\omega_s)$, and the bare dissipation rate $\gamma=\pi|g|^2$. Note that, for a computation of the transmission amplitude $\mathcal{T}$ one can use Eqs. (30) and (31) with $\langle\tilde{\sigma}_-\rangle\to\langle\tilde{\sigma}_-^{(g)}\rangle$.

Unlike in the two-level system, dissipation rates of the Λ system depend on multiple parameters. At fixed γ, the smallest dissipation rate $\gamma_{\min}$ has a nearly quadratic parametric dependence on the drive amplitude F, as shown in Fig. 5. This indicates that we can push the system into the nonadiabatic regime with $\Omega>\gamma_{\min}$ by sweeping the values of F towards zero. Note that $\gamma_{\min}$ shows little sensitivity to the intensity f of the probe field.

In the EIT model with constant $F\neq 0$, the system is fully transparent on resonance $\delta_1=\delta_2=0$ leading to $|\mathcal{T}|^2=1$. When F is momentarily quenched, the metastable state $|s\rangle$ is decoupled for a short while, and the remaining two-level system $\{|g\rangle,|e\rangle\}$ tends to develop full reflection (and, hence, zero transmission), provided that the probe field does not saturate the system. In the next time instant, the state $|s\rangle$ is recoupled again, which leads to nonadiabatic changes in transmission properties. Changing F periodically in time, e.g., by $F(t)=10\gamma[1+\cos\Omega t]$ can thus result in a periodic steady-state behavior of the transmission with large deviations from unity on a single period of modulation. This is illustrated in Fig. 6. Switching between opaqueness and transparency closely resembles the behavior of the two-level system where the modulated coupling effectively performs the function similar to that of F, although with the reciprocal effect. As is seen from the comparison of the adiabatic approximation (dashed line) with the numerical solution (solid line) at $f=\gamma$, the system's response is nonadiabatic during a large part of the period for rather slow modulation frequency $\Omega=0.1\gamma$. This behavior is due to the modulation protocol of F which deeply penetrates into the critical region defined by $\Omega>\gamma_{\min}$ (cf. Fig. 5).

In the high-frequency regime of modulation, the regular EIT effect with unit transmission on resonance is again restored as long as the time average $\bar{F}\neq 0$. For $\bar{F}=0$ we obtain an effective decoupling of the metastable state $|s\rangle$, reproducing the transmission of the unmodulated two-level system. These conclusions are also supported by the high-frequency expansion (23).

VI. DRIVEN KERR-NONLINEARITY SYSTEM

In the third application of our formalism, we consider the driven Kerr-nonlinearity model. It consists of a single cavity

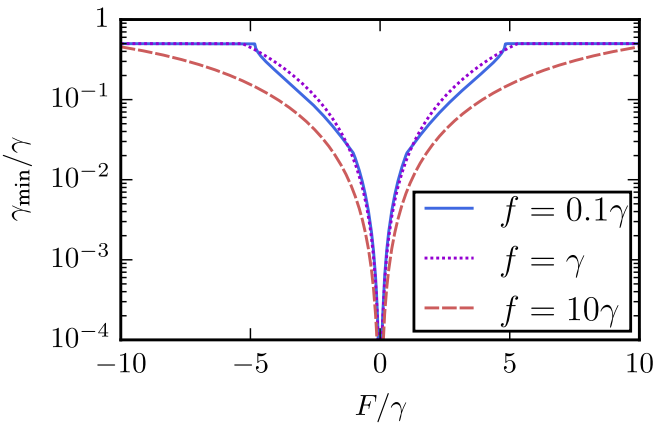

FIG. 5. Smallest dissipation rate $\gamma_{\min}$ of the Λ system as a function of the classical drive field amplitude F. Instead of directly modulating the coupling strength g, the three-level Λ system allows tuning of $\gamma_{\min}$ by means of F. The input power f of the probe field has little effect on this behavior.

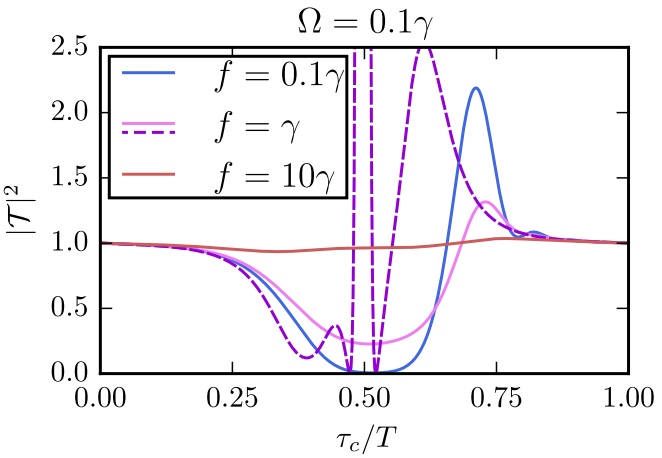

FIG. 6. Transmission through the Λ system which is driven on resonance ($\delta_1 = \delta_2 = 0$) by both probe and drive pulses. The drive field has a periodically modulated amplitude $F(t) = 10\gamma[1 + \cos \Omega t]$ at $\Omega = 0.1\gamma$. The adiabatic approximation (dashed line) is only valid far away from the critical region defined by $\Omega > \gamma_{\min}$ (cf. Fig. 5). In the time window where it breaks down, the system responds nonadiabatically. At large powers f of the probe field, these effects are, however, washed out because of the system's saturation.

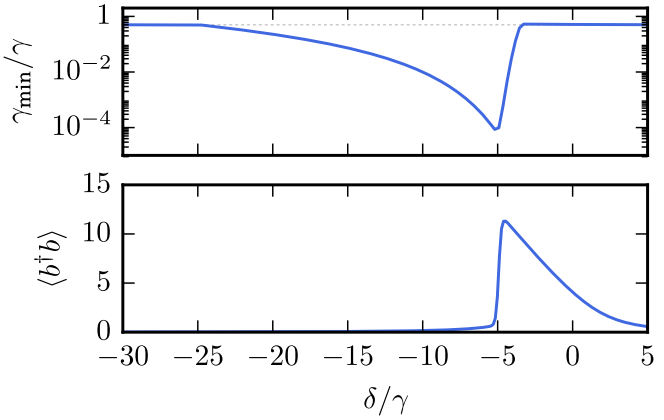

FIG. 7. (top) Smallest dissipation rate $\gamma_{\min}$ of the undriven Kerr-nonlinearity model as a function of detuning δ for $U = -\gamma/2$ and $f = 16\gamma$. Similar to the two- and three-level systems, the smallest dissipation rate is significantly suppressed within the critical region, although it remains finite. (bottom) One of the important signatures of the dissipative phase transition is a prominent increase in the stationary occupation number $\langle b^\dagger b\rangle$ which peaks at the same parameter value for which the minimal dissipation rate is reached. In the following, the periodic modulation of δ is considered across the whole critical region with modulation frequency $\Omega \ll \gamma$.

mode b with an effective local photon-photon interaction U, which is coupled to the transmission line. Its dissipative dynamics in the corotating frame is governed by the Lindblad master equation (3) with $O = b$ and

$$H_{\text{eff}}(t) = -\delta(t) b^\dagger b + \frac{U}{2} b^\dagger b^\dagger b b + \sqrt{\gamma f}(b + b^\dagger). \quad (48)$$

In the following, we consider time-modulation of the detuning $\delta = \omega_0 - \omega_e$, where ω_e is the cavity frequency.

Before turning to the time-dependent case, let us revisit the results obtained by Drummond and Walls [28] and recently extended to include two-photon driving [32] in the time-independent stationary case. The dissipative phase transition that this system exhibits for large $f \gg \gamma$ and small $|U| \ll \gamma$ has numerous manifestations. Experimentally, the most feasible quantity is the stationary occupation $\langle b^\dagger b\rangle$. Sweeping detuning δ over the bistability critical region (i.e., where the corresponding semiclassical solution has multiple solutions), one can observe a strong enhancement in the occupation number (shown in Fig. 7, bottom). Away from this region, $\langle b^\dagger b\rangle$ decays to small values. The peak value rapidly grows with increasing ratio f/U^2. This behavior goes hand in hand with the entropy of the cavity: Outside of the critical region, the state is a pure coherent state corresponding to zero entropy, but becomes a complicated mixed state within the critical region.

This critical behavior can again be attributed to the smallest dissipation rate $\gamma_{\min}$ being significantly suppressed (shown in Fig. 7, top), a phenomenon which is also known as the critical slowing down. In fact, the Liouvillian gap does not completely close. The minimal value of the dissipation is reached at δ where also the occupation number peaks.

Of particular interest is a periodic modulation of parameters which drives the system in and out of the critical region. Recently, it has been proposed [31] that in this way one can dynamically simulate a hysteretic behavior in the Kerr model, which has been experimentally observed [33] in the corresponding setup soon after. Interestingly, the hysteresis-like behavior follows the stable branches of the semiclassical mean-field solution rather than the exact stationary quantum solution. An explanation of this property has been provided in the context of the driven-dissipative Rabi model [27] where it has been shown that long-lived metastable states with a small effective decay rate prevent reaching the true stationary state. As pointed out in Ref. [31], this goes together with a breakdown of adiabaticity, which we have also seen in the previously discussed models. The studies cited above give strong indications that such behavior seems to be common for all systems featuring dissipative phase transitions.

In contrast to modulating f as discussed in Ref. [31], we choose to vary in time the parameter δ. This is advantageous since one can sweep *in* and *out* of the critical region in the positive and negative sweep directions, starting on both sides from noncritical regions characterized by zero values of entropy. In particular, we have found that it is hard to ensure this when sweeping f at fixed δ. Our modulation protocol is designed to cover the whole critical region; namely, $\delta(t) = -15\gamma[1 + \cos \Omega t]$ for the parameters $U = -\gamma/2$ and $f = 16\gamma$.

The periodic steady-state occupation over a single period and its parametric dependence on the parameter δ is shown in Fig. 8. The left panel of Fig. 8 reveals a clear rise in occupation whenever δ is deep inside the critical region, which is followed by an exponential drop. Note that, in comparison with the time-independent stationary state, the occupation is significantly enhanced for intermediate modulation frequency $\Omega = 0.2\gamma$ (dotted line). A further increase of Ω up to the value 2γ does not further enhance the occupancy (solid line); moreover, hysteretic properties are no longer seen in the parametric representation of the right panel of Fig. 8.

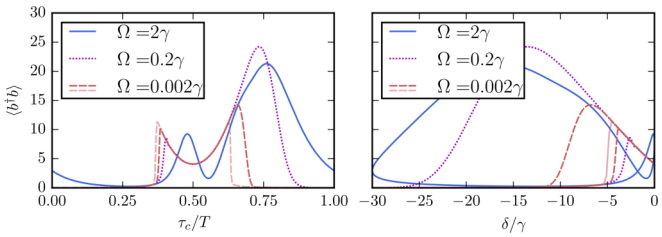

FIG. 8. (left) Periodic steady-state occupation $\langle b^\dagger b\rangle(t)$ of the Kerr-nonlinearity model under periodic modulation of detuning $\delta(t) = -15\gamma[1 + \cos\Omega t]$ for various modulation frequencies Ω. (right) The same dependence in the parametric representation. For moderate modulation frequencies, the occupation is strongly enhanced compared with the true stationary state shown in the lower panel of Fig. 7. The adiabatic approximation based on Eq. (19) is given by the light brown curve (note that in the parametric representation it lies very close to the stationary-state result). The numerical results for rather small frequency $\Omega = 0.002\gamma$ (brown) still drastically deviate from the corresponding adiabatic approximation (light brown). As discussed by Casteels *et al.* [31], the dynamical hysteresis seen in the parametric plot is directly related to the breakdown of adiabaticity in the critical region, and the hysteresis area depends on the width of the parameter range where $\Omega > \gamma_{\min}$.

For slow modulation, the periodic steady-state solution does not converge to the adiabatic approximation based on Eq. (19) (light brown curve) even for $\Omega = 0.002\gamma$. This points towards the nonadiabatic system's response when its parameters are driven across the region of bistability.

VII. SUMMARY

Based on Floquet's theorem, we have proposed a representation for the periodic steady-state density operator of a periodically driven dissipative open quantum system. We have established both adiabatic and high-frequency expansions in a systematic way. Importantly, the corresponding approximations can be efficiently benchmarked against numerical results which are achieved by integration over a single period of modulation. A breakdown of the adiabatic approximation signals the nonadiabatic system's response when it enters the regime of critical slowing down.

We applied the developed formalism to three different models with periodically time-dependent parameters, which all exhibit a temporary suppression of the smallest dissipation rate.

For the two-level system, a modulation of the coupling strength to the transmission line causes significant changes in transmission properties, power spectra, and statistical properties of scattered photons.

For the three-level Λ system, a modulation of the classical driving of the metastable state can lead to considerable modifications of the EIT phenomenon.

In the driven Kerr-nonlinearity model, we studied periodic sweeping of the detuning δ across the parameter region featuring the driven dissipative phase transition. We have found that, even for slow modulation frequencies, nonadiabatic effects dominate, indicating that adiabatic expansions will generally fail in the critical parameter regimes of such systems.

ACKNOWLEDGMENTS

We gratefully acknowledge useful discussions with D. Krimer and M. R. Wegewijs. V.R. is supported by the Deutsche Forschungsgemeinschaft (DFG) under Grant RTG 1995. The work of V.G. is part of the Delta-ITP consortium, a program of the Netherlands Organization for Scientific Research (NWO) that is funded by the Dutch Ministry of Education, Culture and Science (OCW).

APPENDIX: DERIVATION OF LINDBLAD MASTER EQUATION

In this appendix, we show how the Lindblad master equation (3) can be derived from the microscopic model defined by the total Hamiltonian (1) and the coupling to the reservoir (2) within the RWA even in the presence of time-dependent modulation.

To this end, consider the Heisenberg equation of motion for the reservoir field operators

$$\dot{a}_{\alpha\omega}(t) = -i(\omega_0 + \omega)a_{\alpha\omega}(t) - \frac{i}{\sqrt{2}}g(t)O(t), \tag{A1}$$

and formally integrate them to obtain

$$a_{\alpha\omega}(t) = e^{-i(\omega_0+\omega)(t-t_0)}a_{\alpha\omega}(t_0) - \frac{i}{\sqrt{2}}\int_{t_0}^{t} dt' e^{i(\omega_0+\omega)(t'-t)}g(t')O(t'). \tag{A2}$$

This solution can now be used to eliminate the reservoir degrees of freedom by inserting it into the Heisenberg equations of motion for the system operators $e_{lm} = |l\rangle\langle m|$ and averaging over the initial state of the reservoir. In fact, the frequency integration appearing in

$$\dot{e}_{lm}(t) = -i[e_{lm}, H_s(t)](t) - i\frac{g(t)}{\sqrt{2}}\left(\sum_\alpha \int d\omega a^\dagger_{\alpha\omega}(t)[e_{lm}, O](t)\right) - i\frac{g^*(t)}{\sqrt{2}}\left([e_{lm}, O^\dagger](t)\sum_\alpha \int d\omega a_{\alpha\omega}(t)\right) \tag{A3}$$

can be performed within the RWA to give a δ function in time,

$$\int d\omega a_{\alpha\omega}(t) = \int d\omega e^{-i(\omega_0+\omega)(t-t_0)}a_{\alpha\omega}(t_0) - \frac{i}{\sqrt{2}}\int d\omega \int_{t_0}^{t} dt' e^{i(\omega_0+\omega)(t'-t)}g(t')O(t') = \sqrt{2\pi}a_{\alpha,\mathrm{in}}(t) - \frac{i\pi}{\sqrt{2}}g(t)O(t), \tag{A4}$$

making explicit the Markovianity of this approximation even in the presence of periodic driving. In the last step, we defined the input field as the Fourier transform of the bare reservoir field in the far past. Analogously, we can also define the output field corresponding to the reservoir field in the far future,

$$a_{\alpha,\mathrm{out}}(t) = \lim_{t_1\to\infty}\frac{1}{\sqrt{2\pi}}\int d\omega e^{-i(\omega_0+\omega)(t-t_1)}a_{\alpha\omega}(t_1) = a_{\alpha,\mathrm{in}}(t) - i\sqrt{\pi}g(t)O(t), \tag{A5}$$

which is needed for the calculation of observables such as reflection and transmission coefficients.

The initial state of the reservoir is considered to be a right-moving coherent wave packet of width d with a mean number of photons $\bar{N}$ corresponding to a photonic flux $f = \bar{N}/d$. This state can be defined via

$$|\Psi_0\rangle = e^{-\bar{N}/2} e^{\sqrt{\bar{N}} b_R^\dagger} |0\rangle, \tag{A6}$$

in terms of normalizable wave-packet operators

$$b_\alpha = \frac{1}{\sqrt{d}} \int_{-d/2}^{d/2} dx a_\alpha(x,t_0) e^{-i\omega_0 x} \tag{A7}$$

from the Heisenberg coordinate representation $a_\alpha(x,t) = \int d\omega a_{\alpha\omega}(t) e^{i\omega x}/\sqrt{2\pi}$. The commutation relations with the wave-packet operator,

$$[a_{\alpha\omega}, b_R^\dagger] = \delta_{\alpha,R} \int_{-d/2}^{d/2} e^{i(\omega_0-\omega)x}/\sqrt{2\pi d}, \tag{A8}$$

imply the action of the input field on the initial state (A6) to be

$$a_{\alpha,\mathrm{in}}(t)|\Psi_0\rangle = \delta_{\alpha,R}\sqrt{f}\,\Theta(d/2 - |t-t_0|)|\Psi_0\rangle. \tag{A9}$$

With this, the Heisenberg equations of motion (A3), when averaged over the initial state $\rho_{\mathrm{tot}}(t_0) = \rho(t_0) \otimes |\Psi_0\rangle\langle\Psi_0|$, become

$$\begin{aligned}\langle \dot{e}_{lm}(t)\rangle &= \mathrm{Tr}[\dot{e}_{lm}(t)\rho_{\mathrm{tot}}(t_0)] \\ &= \langle m| -i[H_{\mathrm{eff}}(t), \rho(t)] + \gamma(t)\mathcal{D}[O]\rho(t)|l\rangle,\end{aligned} \tag{A10}$$

where the effective Hamiltonian $H_{\mathrm{eff}}(t)$ and the Lindblad dissipator $\mathcal{D}[O]$ are specified by Eqs. (4) and (5), respectively, and follow from switching back to the Schrödinger picture. The Lindblad master equation (3) can be directly identified by the matrix elements $\dot{\rho}_{ml} = \langle \dot{e}_{lm}\rangle$ of the reduced density operator.

[1] G. Floquet, Sur les équations différentielles linéaires a coefficients périodiques, Ann. Ec. Norm. Suppl. **8**, 3 (1879).

[2] F. Bloch, Über die quantenmechanik der elektronen in kristallgittern, Z. Physik **52**, 555 (1929).

[3] Ya. B. Zel'dovich, The quasienergy of a quantum-mechanical system subjected to a periodic action, Zh. Eksp. Teor. Fiz. **51**, 1492 (1967) [Sov. Phys. JETP **24**, 1006 (1967)].

[4] J. H. Shirley, Solution of the schrödinger equation with a hamiltonian periodic in time, Phys. Rev. **138**, B979 (1965).

[5] S.-I. Chu, Recent developments in semiclassical Floquet theories for intense-filed multiphoton processes, Adv. At. Mol. Phys. **2**, 197 (1985).

[6] N. L. Manakov, M. V. Frolov, A. F. Starace, and I. I. Fabrikant, Interaction of laser radiation with a negative ion in the presence of a strong static electric field, J. Phys. B: At., Mol. Opt. Phys. **33**, R141 (2000).

[7] S.-I. Chu and D. A. Telnov, Beyond the Floquet theorem: Generalized Floquet formalisms and quasienergy methods for atomic and molecular multiphoton processes in intense laser fields, Phys. Rep. **390**, 1 (2004).

[8] M. Grifoni and P. Hänggi, Driven quantum tunneling, Phys. Rep. **304**, 229 (1998).

[9] B. Ya. Zel'dovich, A. M. Perelomov, and V. S. Popov, Relaxation of a quantum oscillator in the presence of an external force, Zh. Eksp. Teor. Fiz. **57**, 196 (1970) [Sov. Phys. JETP **30**, 111 (1970)].

[10] J. Cayssol, B. Dóra, F. Simon, and R. Moessner, Floquet topological insulators, Phys. Status Solidi RRL **7**, 101 (2013).

[11] V. Khemani, A. Lazarides, R. Moessner, and S. L. Sondhi, On the Phase Structure of Driven Quantum Systems, Phys. Rev. Lett. **116**, 250401 (2016).

[12] M. Aidelsburger, S. Nascimbene, and N. Goldman, Artificial gauge fields in materials and engineered systems, arXiv:1710.00851.

[13] T.-S. Ho, K. Wang, and S. I. Chu, Floquet-Liouville supermatrix approach: Time development of density-matrix operator and multiphoton resonance fluorescence spectra in intense laser fields, Phys. Rev. A **33**, 1798 (1986).

[14] S. Kohler, T. Dittrich, and P. Hänggi, Floquet-Markov description of the parametrically driven, dissipative harmonic quantum oscillator, Phys. Rev. E **55**, 300 (1997).

[15] B. Roche *et al.*, A two-atom electron pump, Nat. Commun. **4**, 1581 (2013).

[16] K. Szczygielski and R. Alicki, Markovian theory of dynamical decoupling by periodic control, Phys. Rev. A **92**, 022349 (2015).

[17] S. Kohler, J. Lehmann, and P. Hänggi, Driven quantum transport on the nanoscale, Phys. Rep. **406**, 379 (2005).

[18] E. B. Davies and H. Spohn, Open quantum systems with time-dependent Hamiltonians and their linear response, J. Stat. Phys. **19**, 511 (1978).

[19] H. P. Breuer and F. Petruccione, Dissipative quantum systems in strong laser fields: Stochastic wave-function method and Floquet theory, Phys. Rev. A **55**, 3101 (1997).

[20] K. Szczygielski, D. Gelbwaser-Klimovsky, and R. Alicki, Markovian master equation and thermodynamics of two-level system in strong laser field, Phys. Rev. E **87**, 012120 (2013).

[21] K. Szczygielski, On the application of Floquet theorem in development of time-dependent Lindbladians, J. Math. Phys. **55**, 083506 (2014).

[22] C. M. Dai, Z. C. Shi, and X. X. Yi, Floquet theorem with open systems and its applications, Phys. Rev. A **93**, 032121 (2016).

[23] K. Brandner and U. Seifert, Periodic thermodynamics of open quantum systems, Phys. Rev. E **93**, 062134 (2016).

[24] R. Kosloff, Quantum thermodynamics: A dynamical viewpoint, Entropy **15**, 2100 (2013).

[25] M. P. Silveri, J. A. Tuorila, E. V. Thuneberg, and G. S. Paraoanu, Quantum systems under frequency modulation, Rep. Prog. Phys. **80**, 056002 (2017).

[26] M.-J. Hwang, P. Rabl, and M. B. Plenio, Dissipative phase transition in the open quantum Rabi model, Phys. Rev. A **97**, 013825 (2018).

[27] A. Le Boité, M.-J. Hwang, and M. B. Plenio, Metastability in the driven-dissipative Rabi model, Phys. Rev. A **95**, 023829 (2017).

[28] P. D. Drummond and D. F. Walls, Quantum theory of optical bistability. I. Nonlinear polarisability model, J. Phys. A: Math. Gen. **13**, 725 (1980).

[29] Z. Leghtas *et al.*, Confining the state of light to a quantum manifold by engineered two-photon loss, Science **347**, 6224 (2015).

[30] W. Casteels, R. Fazio, and C. Ciuti, Critical dynamical properties of a first-order dissipitave phase transition, Phys. Rev. A **95**, 012128 (2017).

[31] W. Casteels, F. Storme, A. Le Boité, and C. Ciuti, Power laws in the dynamic hysteresis of quantum nonlinear photonic resonators, Phys. Rev. A **93**, 033824 (2016).

[32] N. Bartolo, F. Minganti, W. Casteels, and C. Ciuti, Exact steady state of a Kerr resonator with one- and two-photon driving and dissipation: Controllable Wigner-function multimodality and dissipative phase transitions, Phys. Rev. A **94**, 033841 (2016).

[33] S. R. K. Rodriguez *et al.*, Probing a Dissipative Phase Transition via Dynamical Optical Hysteresis, Phys. Rev. Lett. **118**, 247402 (2017).

[34] D. R. Dion and J. O. Hirschfelder, Time-dependent perturbation of a two-state quantum system by a sinusoidal field, Adv. Chem. Phys. **35**, 265 (1976).

[35] H.-I. Yoo and J. H. Eberly, Dynamical theory of an atom with two or three levels interacting with quantized cavity fields, Phys. Rep. **118**, 239 (1985).

[36] M. Bukov, L. D'Alessio, and A. Polkovnikov, Universal high-frequency behavior of periodically driven systems: From dynamical stabilization to Floquet engineering, Adv. Phys. **64**, 139 (2015).

[37] M. Pletyukhov, K. G. L. Pedersen, and V. Gritsev, Control over few-photon pulses by a time-periodic modulation of the photon emitter coupling, Phys. Rev. A **95**, 043814 (2017).

[38] R. Barends *et al.*, Digitized adiabatic quantum computing with a superconducting circuit, Nature (London) **534**, 222 (2016).

[39] L. Viola, E. Knill, and S. Lloyd, Dynamical Decoupling of Open Quantum Systems, Phys. Rev. Lett. **82**, 2417 (1999).

[40] C. Gustin, R. Manson, and S. Hughes, Spectral asymmetries in the resonance fluorescence of two-level systems under pulsed excitation, Opt. Lett. **43**, 779 (2018).

[41] O. A. Kocharovskaya and Ya. I. Khanin, Population trapping and coherent bleaching of a three-level medium by a periodic train of ultrashort pulses, Zh. Eksp. Teor. Fiz. **90**, 1610 (1986) [Sov. Phys. JETP **63**, 945 (1986)].

[42] K.-J. Boller, A. Imamoglu, and S. E. Harris, Observation of Electromagnetically Induced Transparency, Phys. Rev. Lett. **66**, 2593 (1991).

[43] A. A. Abdumalikov, Jr., O. Astafiev, A. M. Zagoskin, Y. A. Pashkin, Y. Nakamura, and J. S. Tsai, Electromagnetically Induced Transparency on a Single Artificial Atom, Phys. Rev. Lett. **104**, 193601 (2010).